Chapter 4

A Novel Principal Component-Based Virtual Sensor Approach for Efficient Classification of Gases/Odors

4.1 Abstract

Real-time applications requiring high accuracy to detect and estimate hazardous gases/odors are too challenging to implement with traditional approaches. Being inspired by the world-known efficacy of Convolutional Neural Networks (CNNs), researchers have started to use CNNs for developing efficient electronic noses (e-Noses). However, the generalization has not been discussed so far to apply CNNs for gas classification independent of types of gas sensor array responses. Recently published works discuss the application of CNNs to classify the gases/odors using only dynamic

responses. No one has conceptualized the applicability of CNN to static responses of gas sensor arrays. Furthermore, while dealing with the drift-free gas sensor array responses, two-dimensional CNNs (2D-CNNs) have been better for classifying the gases/odors. However, 2D-CNN performs better when they operate on a two-dimensional data vector of minimal size with suitable size of kernels. In this chapter, we will discuss an approach to utilizing 2D-CNN for gas classification using steady-state responses of the gas sensor array. In this regard, the operational data vectors are augmented with the synergy of mirror mosaicking and padding of virtual sensor responses. In our work, the principal components of physical gas sensor responses have been used as virtual responses that work better than traditional zero-padded virtual sensor responses. Two sets of data have been upscaled to demonstrate the experimental results with this approach. Since the upscaled datasets consist of physical and virtual sensor responses, they have been called hybrid datasets throughout the chapter. With this, a simpler 2D-CNN achieves 100 percent correct classification in two different experimental settings corresponding to two datasets. To the best of our knowledge, we are the first to utilize a principal component-based hybrid, the upscaled dataset. An e-Nose designed with this approach can achieve 100 percent correct classification for the considered gases/odors.

4.2 Introduction

The real-time applications of gas sensing systems are crucial for detecting and estimating gases/odors in industrial and social paradigms [179, 180]. These gas sensing systems are popularly known as electronic noses (e-Noses); their comprehensive list of applications can be seen in [181, 182]. The primitive applications of e-Noses have used traditional pattern recognition techniques. In contrast, the e-Nose in

current scenarios uses Artificial Intelligence (AI)-based advanced approaches such as Convolutional Neural Networks (CNNs) to mimic the human olfactory system. Traditional techniques for pattern recognition, such as statistical and probabilistic methods, highly depend on some assumptions and data pre-processing creating bottlenecks for real-time implementations [152]. A classical statistical way is K-nearest neighbor (KNN), which requires the whole training data at each calculation. Hence, it needs storage of training data exerting space complexity and hindering its real-time implementation [162]. In contrast, real-time gas/odor classification can be implemented suitably using AI-based approaches [179, 180, 183]. A schematic for AI-based gas sensing systems or Intelligent Gas-Sensing Systems (IGS) is depicted in Fig. 4.1(a). This figure shows that a typical IGS requires pre-processed or normalized raw sensor array responses to classify the considered gases/odors. The traditional pattern recognition techniques can classify/quantify the considered gases/odors efficiently only using pre-processed data. Subsequently, our proposed AI-based IGS utilizing hybrid analysis space (raw and virtual sensor responses) has been shown in Fig. 4.1(b).

Typically, both dynamic and static responses of gases are captured using the gas sensor array. And a gas sensor array in each IGS system consists of a few (generally, 4 to 16) gas sensor elements [163, 184–188]. IGS systems or efficient e-Noses are being developed using advanced neural networks like CNN in the current scenario.

A 2D deep CNN has been tailored as "GasNet" to classify the gases/odors, viz., carbon monoxide, ethylene, hydrogen, and methane [162]. It has a relatively complex architecture comprising six convolutional blocks or 38 layers as a whole. While classifying the considered gases/odors, they used 1200 data vectors for training and testing of GasNet using a ratio of 70/30 percent, where each data vector

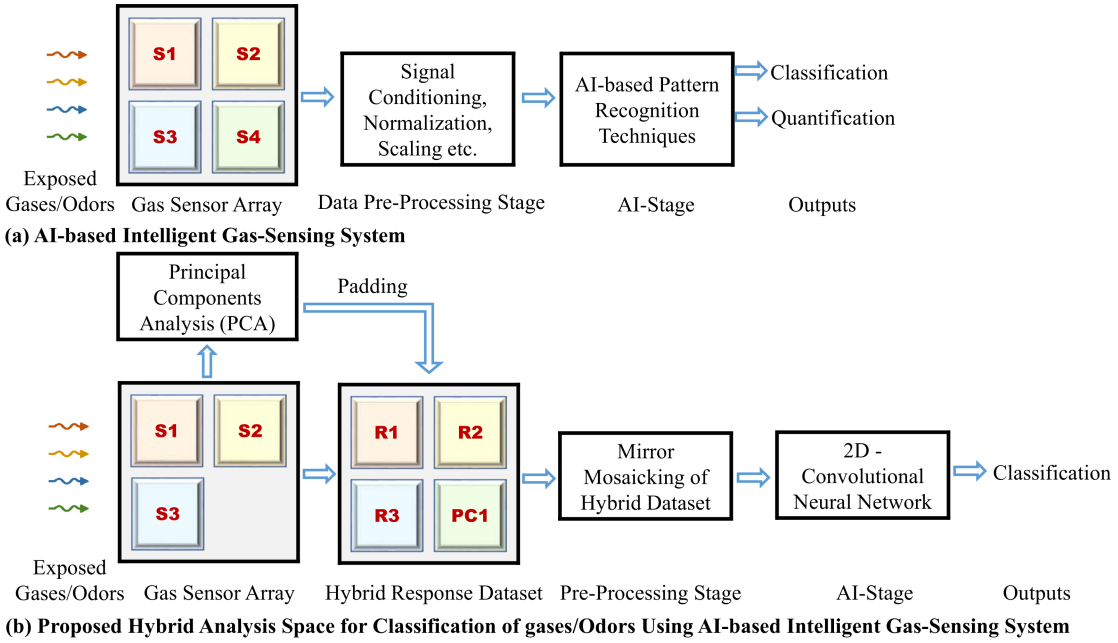

FIGURE 4.1: (a) AI-Based Intelligent Gas-Sensing (IGS) System, (b) AI-Based IGS System Utilizing Hybrid Analysis Space

consists of 8000 data points. They achieved a 95.20 percent recognition rate during the experiment, successfully. Moreover, a LeNet-5 [167]-based 2D CNN was developed by Wei et al. (2019) to classify carbon monoxide, methane, and its mixture [164]. They achieve a recognition rate of 98.67 % for gas/odor classification using 1000 vectors for training and testing in the ratio of 80/20 percent, where each sample has a size of 12 $\times$ 480 data points. Furthermore, in [188], authors have used standard CNN architectures (e.g., VGG-16,19, and ResNet-18,34,50) to classify three considered gases/odors (e.g., carbon monoxide, ethylene, methane) and their two binary mixtures. With the data vectors of size (8 $\times$ 3000), the authors apply a 5:1 train-test split on original data having 540 samples. They achieved the best recognition rate of 96.67 % following this data division.

So far, all the discussed works only use 1D or 2D representation of data vectors obtained from dynamic responses. Such data vectors embrace high dimensionality because of the high sampling rate and significant sampling duration. In

fact, high dimensionality leads to computational complexity. In contrast, the static (steady-state) responses evidently have the least possible dimensionality, leading to computationally efficient data processing in gas sensing. The steady-state responses of metal oxide (MOX)-based non-selective gas sensors are referred to as the golden response of a gas sensor array [189, 190]. In real-field applications of gas sensing, dynamic responses cannot identify analyte concentrations under observation. In contrast, they can classify the gases/odors exposed to the gas sensor array. It is evident from the reviewed publications that the authors utilized both dynamic and static responses simultaneously. With this fact, the data to be processed becomes of high dimensionality. Obtaining the desired performance with this high-dimensional data shows a low utilization factor, i.e., high performance on utilizing extensive data accumulating both dynamic and static responses. Moreover, the combined high-dimensional data require relatively complex CNN architectures [162, 164, 188].

To strengthen the utilization factor, we have proposed a novel approach that provides high performance using merely static responses. Our policy reduces the optimal size of input vectors to the number of gas sensor elements in the array. In this regard, the ideal steady-state responses are approximated by taking the average of corresponding static responses. Also, our proposed approach reduces the sizes of input sample vectors from $8 \times 600 \times 100$ to 8×1 and $5 \times 300 \times 25$ to 5×1, respectively, for the considered two datasets. Further, considering that spatial features are more salient than temporal features, 1D data vectors have been upscaled to 2D data structures for automatic information extraction using the inherent capability of a 2D-CNN. Accordingly, the intermediate conversion stages of data vectors have been shown in Table 4.1. Moreover, the process of upscaling the 1D data vectors into the 2D array follows two steps: padding of virtual sensor responses (zero or non-zero) and spatial augmentation using mirror mosaicking.

TABLE 4.1: Intermediate Steps in Data Vector Conversion Process

$\Downarrow \Longrightarrow$	Dataset-1	Dataset-2
Raw Data Vectors ($N \times S_d \times S_r$)	$8 \times 600 \times 100$	$5 \times 300 \times 25$
Averaged Static Responses	8×1	5×1
Hybrid Data Vectors	9×1	9×1
1D to 2D Representation	3×3	3×3
Spatially Augmented Data Vectors	9×9	9×9
$N : GasSensorElements, S_d : SamplingDuration(s), S_r : SamplingRate(H_z)$		

4.3 Methodology

4.3.1 Characteristics of Gas Sensor Array Responses

A typical gas sensor array consists of several MOX-based gas sensor elements that have been designed to detect a broad range of analytes (non-selective) depending on their varying fabrication parameters. These gas sensing elements are fabricated through the doping mechanism. The gas sensor array comprising such gas sensing elements is interfaced with various hardware modules capable of acquiring data using different sampling frequencies. The characteristic response of one of the activated gas sensors on exposing the gas/odor is shown in Fig. 4.2.

The dotted horizontal line represents the baseline resistance (see Fig. 4.2). Whereas decaying and rising steeps show the drop and increment in resistance proportional to the affinity of the exposed analyte to the sensing element. The decaying steep proportionately shows the growing concentration. In contrast, the rising resistance shows the recovery phase. These varying curves correspondingly result in dynamic or transient responses of the gas sensor array. Moreover, the variation in resistance curves becomes approximately static between the decaying and recovery (or rising and recovery for N-type Metal Oxide Semiconductor) phase. Thereby, the average of these static responses is assumed to be steady-state since the ideal

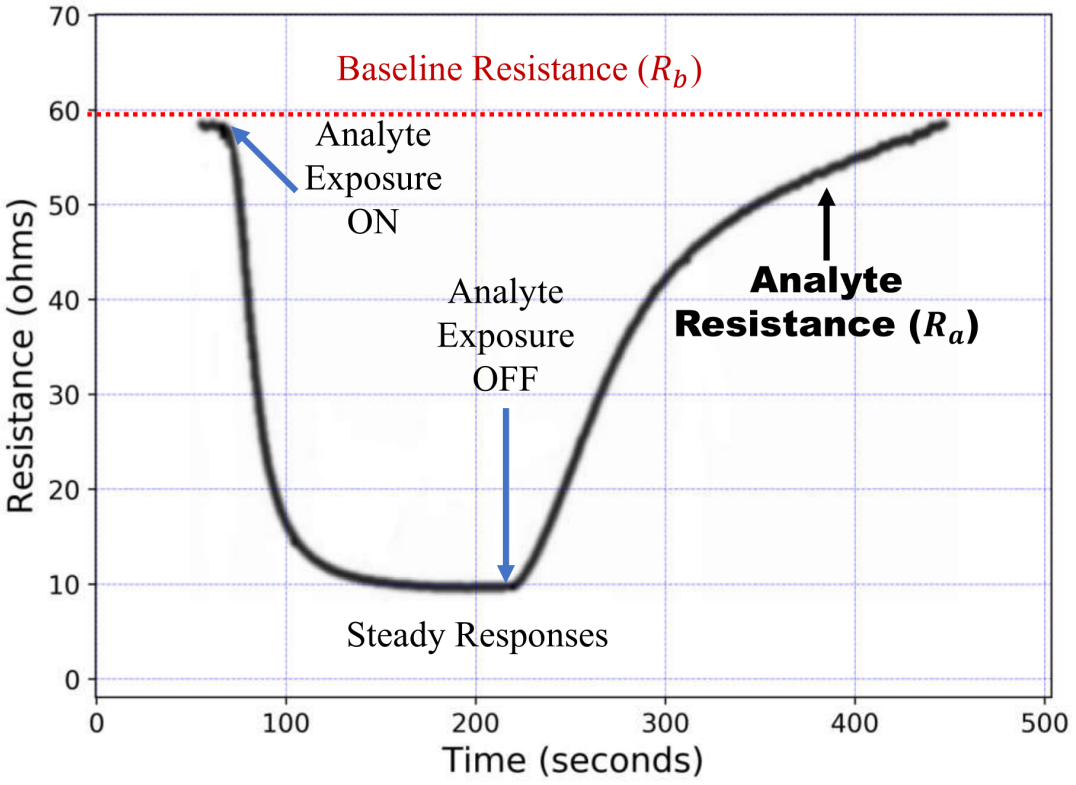

FIGURE 4.2: Response Characteristics of MOX-Based Gas Sensing Element During Exposure of Analyte (Gas/Odor)

steady-state is typically achieved at an infinite instance of time. Mathematically, the steady-state values of resistance are measured as percentage changes with baseline resistance. Such steady-state values result in the least possible data vector with a size equal to the number of gas sensor elements in the gas sensor array. At the same time, the size of data vectors that are achieved through the dynamic responses has a significantly large size depending on the sampling rate and duration. The transient responses represent only class-specific information, while steady-state responses are capable of representing class-specific as well as concentration-proportional information. Hence, the steady-state responses are referred to as the gold standards for a gas sensor array. Regarding Table 3.1, we have used two publicly available datasets. Accordingly, the steady-state responses are first extracted from the corresponding

mixed (dynamic and static) responses for 640 and 58 samples, respectively. In this way, the huge-sized raw data vectors are downsampled from $8 \times 600 \times 100$ to 8×1 and $5 \times 300 \times 25$ to 5×1, respectively.

4.3.2 Upscaling Through Virtual Sensor Responses

A 2D-CNN can operate on multidimensional (2D or 3D) input data vectors to extract salient features. It inherently limits the size of input data vectors following the size of kernels used for linear convolution operation. For illustration, 3×3 kernels require input data vectors larger than themselves for efficient extraction of features. We extract steady-state response data vectors as discussed earlier. These are to be upscaled for the smooth operation of 2D-CNN. This upscaling is processed using two steps: padding virtual sensor responses and mirror mosaicking. Each data vector requires virtual sensor responses so that the total of physical and virtual sensor responses approaches the nearest perfect square number. It is inevitably necessary to convert the raw 1D input data vectors into 2D-squared data vectors. Hence, if the gas sensor array does not has sensing elements equal to a perfect square number, additional virtual sensor responses need to pad the actual sensor responses. Typically, zero-padding is found to be a popular scheme for various objectives based on padding [191–194]. However, the zero-padding does not provide significant values that may contribute to the information content. With this inference, we have proposed a novel scheme of padding with non-zero values that not only enhance the required size of data vectors but also boosts the performance of pattern recognition tasks. In this approach, the role of virtual sensor responses has been demonstrated with the help of Fig. 4.3. It is also evidently shown that the total of both genuine and virtual sensor elements approaches the nearest perfect square number.

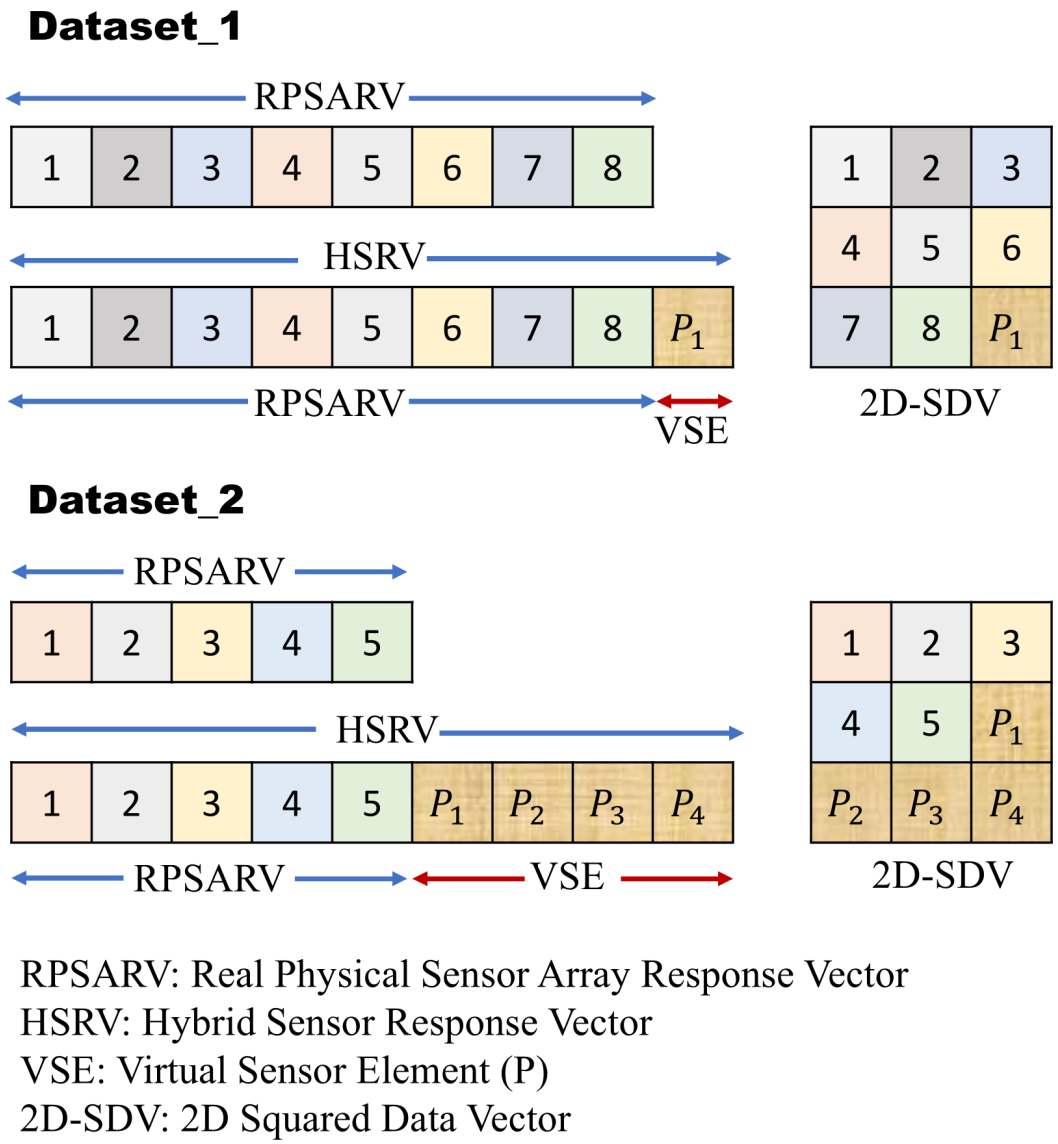

FIGURE 4.3: The Explained Role of Virtual Sensor Responses

4.3.3 Techniques for Virtual Sensor Responses

As of discussion, we require virtual sensor responses to fulfill the requirement of the first step of upscaling. In the second step, mirror mosaicking requires 2D-squared input data vectors that depend on the first step. Since it is not always sure that the number of gas sensor elements in the gas sensor array is equal to the perfect square number, if done knowingly, redundancy will also be increased with the number of

sensor elements. More sensor elements in the array result in relatively high cost, high power consumption, and more space on the hardware platform. Also, if data points in the input data vectors are not equal to a perfect square, it is impossible to convert a 1D data vector into a 2D-squared data vector. Hence, we have used utilized the significance of virtual sensor responses. The virtual sensor responses are derived from physical sensor responses. Mishra et al. (2017) in [165] reported several techniques for generating virtual sensor responses. Thus, the obtained virtual sensor responses are then appended one by one to the physical sensor responses until the total count of responses becomes a perfect square number. After padding the virtual sensor responses, a new data vector consisting of physical and virtual elements has been referred to as a hybrid data vector. The construction of a hybrid data vector is well represented in Fig. 4.3. From this figure, it is also evident that we have first pad the virtual sensor responses (with zero or non-zero values) in the raw input data vectors to make the hybrid data vectors, which can be restructured further into 2D-squared data vectors.

4.3.4 Zero and Non-Zero Padding

The conventional zero-padding inserts zeroes wherever it is applied. In contrast, non-zero padding schemes use different non-zero values for padding depending on the utilized algorithm. The usage of padding in the context of the work presented here can be understood as follows. For illustration, assume the gas sensors' responses have been recorded using a gas sensor array employing n sensor elements. Thus, the obtained corresponding steady-state responses have n data points in each input data vector resulting from n physical gas sensors. Depending on the number of physical gas sensors, two following possibilities are there:

1. n is a perfect square number that can be denoted as $x \times x = n$, where x is a positive integer. In this case, no padding of virtual sensor response is required to implement the first step of input data vector upscaling.

2. n is not a perfect square number. In this case, the padding of some virtual sensor responses is required to make the total count of elements from physical and virtual sensor responses equal to a perfect square number. Without padding, n never be denoted as $x \times x = n$, where x stands for a positive integer. Suppose $(p - n)$ virtual sensor responses are needed for padding, where p is the smallest perfect square number to n such that $p > n$. After padding the required virtual sensor responses, p can surely be represented as $y \times y = p$, where y stands for a positive integer.

The required non-zero virtual sensor responses depend on the algorithm used to calculate. For example, six virtual sensor responses can be generated using four physical sensor responses using NDSRT [165]. The efficacy of such generated virtual sensor responses depends on the used technique, but they counter an issue of virtual sensor response selection as per requirement. Hence, we require an algorithm capable of resulting in sorted virtual sensor responses. Accordingly, we can select virtual senor responses as per our requirements. Principal Components Analysis (PCA) is a popular technique that results in principal components sorted through explained variance. Only a few principal components can represent almost 95% of the information content of the raw data [195]. Therefore, we have used this salient nature of PCA to generate non-zero virtual sensor responses as per our work's requirement. We are the first to use the inference of PCA in this kind of application. Thus, with this novel approach, the obtained hybrid data vectors are further upscaled to train a 2D-CNN. Such trained CNNs are capable of providing outperforming results.

4.3.5 Mathematical Ground of Principal Component Analysis

The Principal Component Analysis (PCA) follows some mathematical and statistical formulations. To illustrate the working of PCA, we are presenting generalized expressions. Suppose X is a dataset containing N recorded samples resulting from S variables. Now, each data point in each data vector of the dataset X can be denoted as $x_{i,j} \in X : \forall i = 1, 2, ..., N \& j = 1, 2, ..., S$. The whole dataset X is transformed to be centered on the origin by subtracting the mean of each variable S. The mean to each variable S is determined as $\mu_j : \forall j = 1, ..., S$. With this transformation, we achieve an origin-centered dataset X' where $x'_{i,j} = (x_{i,j} - \mu_j)$. Subsequently, the covariance matrix from this transformed dataset X' is determined as $C_{X'} = \frac{1}{(N-1)} X' X'^T$. Further, the eigenvalues and eigenvectors of this covariance matrix are determined. The eigenvectors are sorted in descending order corresponding to the eigenvalues. Next, D eigenvectors are arranged column-wise for D sorted eigenvalues to obtain a projection matrix V, where the elements can be represented as $v_{i,j}$. This projection matrix V consists of D independent eigenvectors. Consequently, desired principal components (PCs) are determined by projecting the X' on V. The corresponding PCs are achieved following the expression $PC_i = x'_{i1} v_{i1} + x'_{i2} v_{i2} + ... + x'_{ij} v_{ij}$ where $\forall x'_{ij} : i = 1, ..., N \& j = 1, ...S; \forall v_{i,j} : i = 1, ..., S \& j = 1, ..., D$. Thus, the obtained PCs are used as virtual sensor responses as per our requirement. They are appended (padded) with physical sensor responses to obtain hybrid data vectors. Such hybrid data vectors are then converted into a 2D-squared input data vector. These modified 2D data vectors are further upscaled using mirror mosaicking.

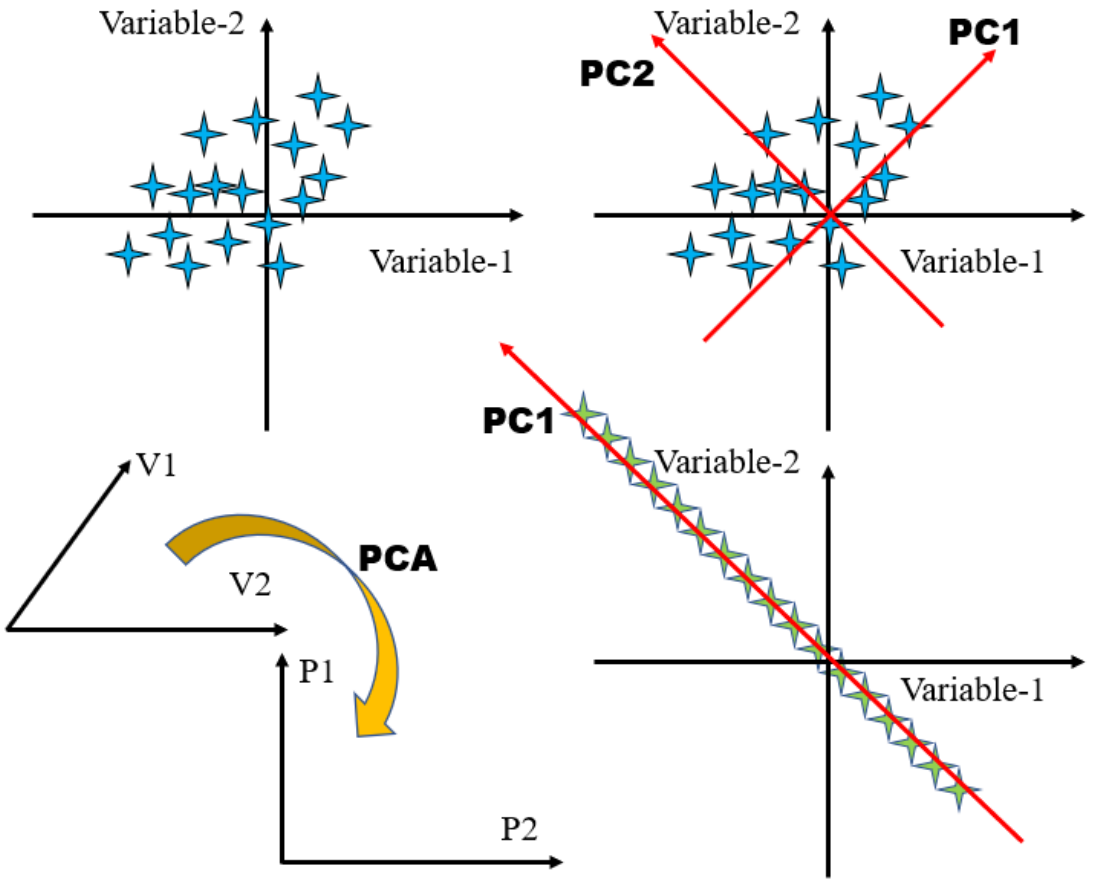

FIGURE 4.4: Graphical Notion of Principal Component Analysis: PCA orthonormalizes the data along with rotated axes.

4.3.6 Mirror Mosaicking

Mirror mosaicking is a technique suitable for spatial augmentation of any 2D-squared data structure that upscales the data by three times. As discussed earlier, we achieve 1D hybrid data vectors using virtual sensor responses that are further restructured as 2D-squared data vectors. Such 2D-squared data vectors then undergo mirror mosaicking for further upscaling. While implementing mirror mosaicking, eight directional images of the taken 2D-squared data are obtained and mosaicked towards

the corresponding directions, viz., W(est)-E(ast)-N(orth)-S(outh)-NW(north-west)-SE(south-east)-SW(south-west)-NE(north-east). The visual support of mirror mosaicking with the illustrations using zero and non-zero padding has been shown in Fig. 4.5(a)-(b). This figure illustrates the mirror mosaicking on a 2D-squared data structure of size (2×2). In Fig. 4.5(a)-(b), 1 and 2 denote the elements of physical sensor responses while 3 and 4 denote padded elements from virtual sensor responses, respectively. Interestingly, the non-zero elements of virtual sensor responses represent more significant information than zero-padded elements.

4.3.7 Architecture of Used 2D Convolutional Neural Network

A 2D-CNN is trained using augmented 2D hybrid input data to classify the considered gases/odors. As discussed earlier, two different datasets have been used and referred to as dataset-1 and dataset-2. Finally, both the upscaled dataset results in input data with a size of (9×9) that are used to train the CNN. Fig. 4.6(a) shows the general architecture of a 2D-CNN. It consists of several convolutional and pooling layers followed by the fully-connected layers signifying a typical multi-layer perceptrons (MLP) neural network. Also, CNNs have pooling layers, especially for image processing applications, because adjacent pixels are highly correlated. In contrast, the pooling layers are not necessarily required to classify the gases/odors since steady-state responses are significantly independent. Hence, we have simplified the typical CNN architecture, as shown in Fig. 4.6(b), to serve the purpose of gas/odor classification. Thus, the simplified 2D-CNN architecture takes the augmented 2D-hybrid input data vectors for its training that carry significantly enhanced information due to the non-zero PCA-based virtual sensor responses. The input data, being rich in information, can be classified using only a few layers. Thereby, utilized

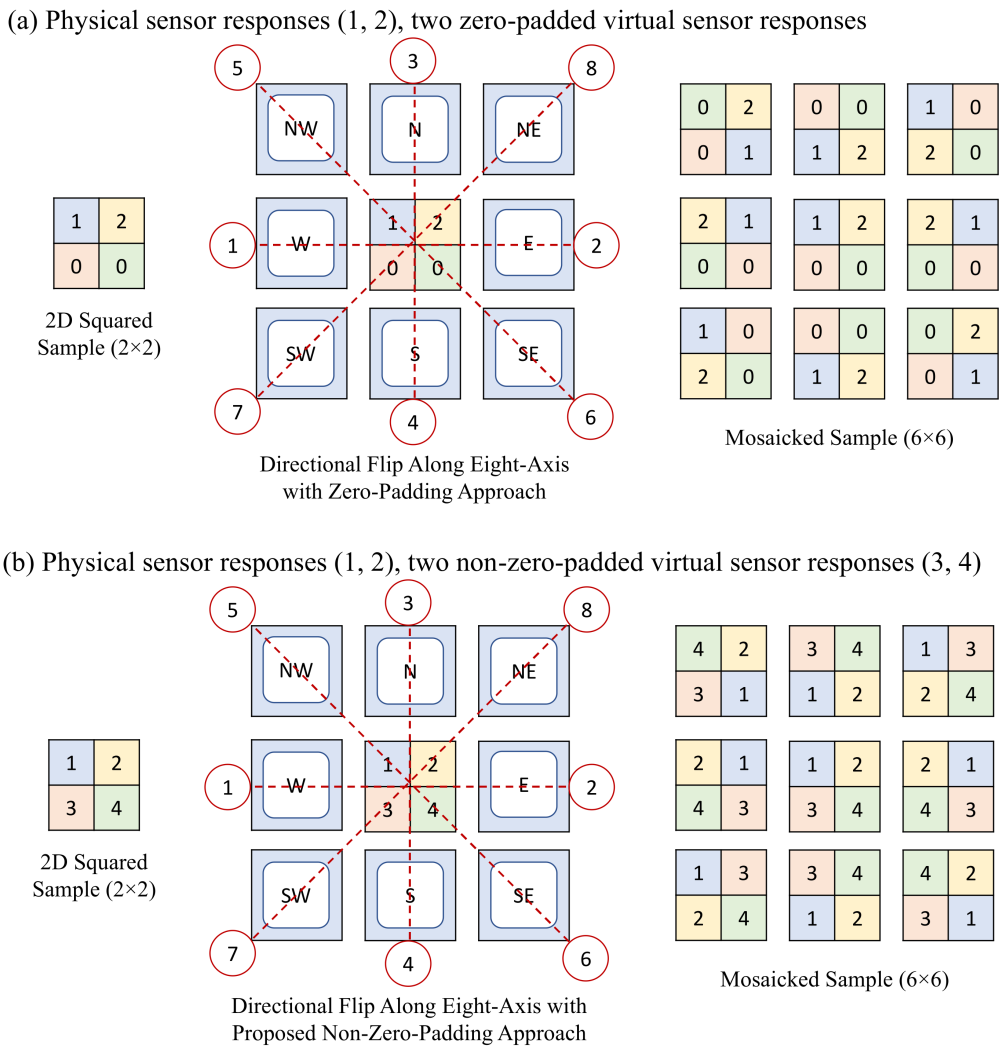

FIGURE 4.5: Mirror Mosaicking Utilizing: (a) Zero-Padding Based Virtual Sensor Responses, (b) Non-Zero Virtual Sensor Responses

simplified CNN architecture consists of only five layers. The first two convolutional layers extract salient features from the input data. The outcomes from the second convolutional layer are forwarded to a fully connected layer. Eventually, the fully-connected layer sends its products to the softmax layer that provides classified results for the considered gases/odors. Moreover, the parameters used in 2D-CNN have been mentioned in Table 4.2.

(a) Typical configuration for a 2D-CNN.

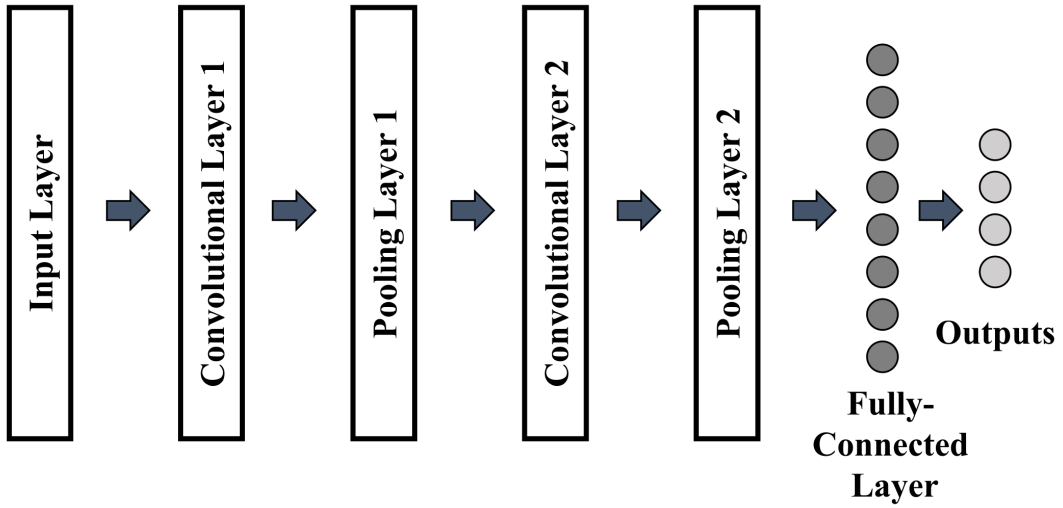

(b) Proposed configuration for a simpler 2D-CNN.

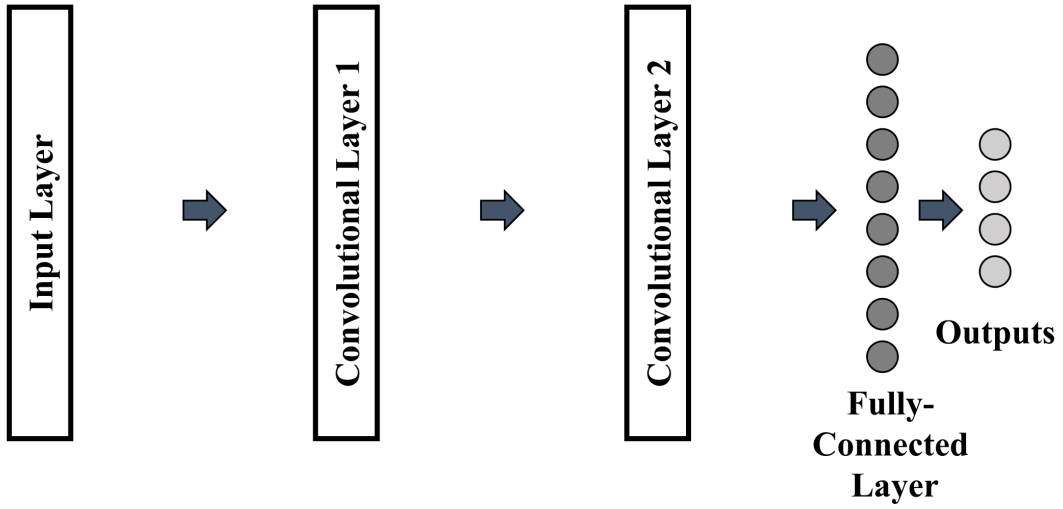

FIGURE 4.6: 2D-CNN Architectures (a) A General Reprsentation, (b) Simplified for Classification of Gases/Odors

4.4 Gas Sensor Array Responses

As quoted earlier, the demonstration of the proposed methodology has been shown using two different datasets. These datasets have been captured from two different gas sensor arrays and referred to as dataset-1 and dataset-2 throughout the chapter.

TABLE 4.2: Parameters Used by Simpler 2D-CNN

Simplified 2D-CNN Layers	Parameter Labels	Parameter Values
Input Layer	Input Dimnesion	$9 \times 9 \times 1$
First Convolutional Layer	Kernel/Filter Dimension	3×3
	No. of Kernels	8
Second Convolutional Layer	Kernel/Filter Dimension	3×3
	No. of Kernels	16
Fully-Connected Layer OR Dense Layer	No. of Neurons	32
Output Layer	Softmax Function	4
Optimizer	Adam	Learning Rate 0.001

4.4.1 Dataset-1

In our work, the utilized dataset-1 has been downloaded from a repository that provides a variety of machine learning datasets for academic purposes [169]. Dataset-1 consists of gas sensor array responses captured on exposing four considered gases/odors. These gases/odors are carbon monoxide (CO), ethanol (C_2H_5OH), ethylene (C_2H_4), and methane (CH_4) which have been exposed to gas sensor array at different concentration levels between the ppm range of 25-250, 12.5-125, 12.5-125, and 25-250, respectively. The corresponding gas sensor array employed eight MOX-based gas sensor elements for data acquisition. A total of 640 time-series vectors (160 for each gas/odor) are recorded where each vector of sensor array response is captured for 600 seconds with a sampling rate of 100 Hz [149]. While using dataset-1, ten-fold cross-validation has been used, whereas a ratio of 80%/20% is applied to split the data randomly for training/testing purposes. Accordingly, 512 samples (carbon monoxide-133, ethanol-127, ethylene-131, methane-121) have been used for training. And the rest of the 128 samples (carbon monoxide-27, ethanol-33, ethylene-29, methane-39) are used for testing to evaluate the classifier's (simplified 2D-CNN) performance.

4.4.2 Dataset-2

We have also demonstrated our methodology on another dataset. Dataset-2 has also been taken from the same source as mentioned for Dataset-1. Dataset-2 has been recorded using a gas sensor array consisting of 16 MOX-based gas sensors. However, the 16 sensors, as mentioned earlier elements belong to five different TGS groups made by Figaro Inc. The details of these 16 gas sensor elements are given in Table 4.3. Thereby, observing that all the mentioned gas sensors uniquely represent five different sensing elements, we have considered the first five unique gas sensor elements for our experimental work. Dataset-2 includes the responses of the gas sensor array captured on exposing the two types of gases, viz., ethanol and acetone, and its binary mixer. In Dataset-2, except for two gases and their mixture, responses measured for ambient air are considered as the fourth class. Furthermore, rather than considering the responses for all the sensing elements, we have considered the responses of only the first five unique sensors. Thus, this truncated version of Dataset-2 has been used to implement our methodology. Interestingly, our proposed method achieves outperforming results even using the truncated dataset instead of the whole available dataset. Dataset-2 consists of 58 samples captured for different concentration doses for the considered gases/odors. They include 15, 15, 20, and 8 ethanol, acetone, binary mixer, and ambient air samples. Refer to the work published in [150] for the extensive detail about Dataset-2. Moreover, we manually divided Dataset-2 for training and testing purposes to consider all the variations of the concentration doses. For training and testing purposes, respectively, 39 and 19 samples have been used.

TABLE 4.3: Details of 16 Gas Sensor Elements *w.r.t.* Dataset-2

16 Sensor Elements		Chosen 5 Sensor Elements	
S.No.	TGS Number	S.No. Old/New	TGS Number
1	TGS 2610	1/1	TGS 2610
2	TGS 2610		
3	TGS 2602	3/2	TGS 2602
4	TGS 2600	4/3	TGS 2600
5	TGS 2610		
6	TGS 2611	6/4	TGS 2611
7	TGS 2610		
8	TGS 2620	8/5	TGS 2620
9	TGS 2610		
10	TGS 2620		
11	TGS 2602		
12	TGS 2611		
13	TGS 2610		
14	TGS 2610		
15	TGS 2610		
16	TGS 2600		

4.4.3 PCA Visualization for Dataset-1 and Dataset-2

For visual inspection of cluster separation among the considered classes of gases/odors, the scatter plots for both datasets have been shown in Fig. 4.7. We have used the first three principal components to plot the clusters in a three-dimensional space. This figure shows the overlapping of clusters that makes the classification task more challenging. All the three principal components collectively explain the variance of data up to 90.92 % ($PC1$: 48.05%, $PC2$: 26.18%, $PC3$: 16.69%) for dataset-1, and 99.99 % ($PC1$: 86.37%, $PC2$: 13.54%, $PC3$: 0.08%) for dataset-2.

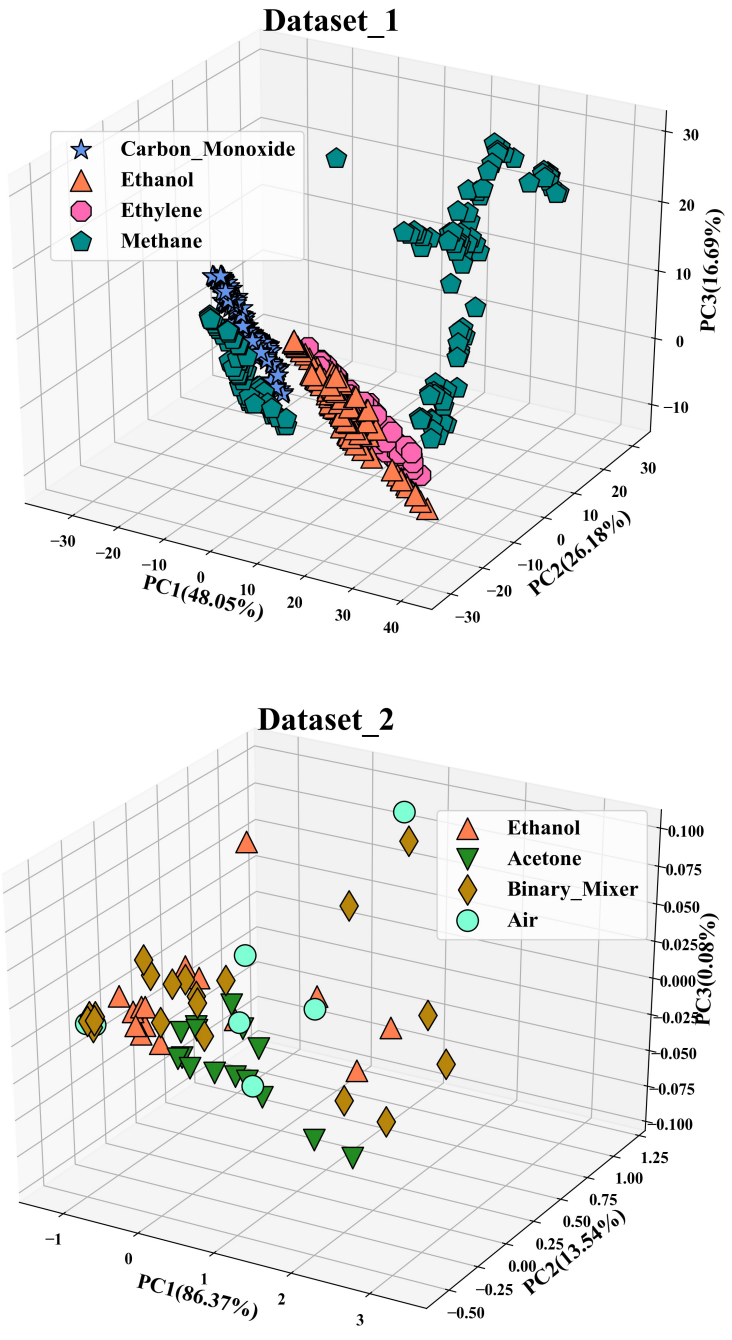

FIGURE 4.7: 3D Cluster Representation for: (a) **UPPER**: Dataset-1, (b) **LOWER** Dataset-2.

4.4.4 Step-wise Description of Approach Implementation

Dataset-1 holds responses captured by eight physical gas sensors. Thereby, making the total count of responses obtained by sensors equal to a perfect square number (i.e., 9), we require padding of one virtual sensor response to demonstrate our methodology. On the other hand, the truncated version of dataset-2 holds responses captured by five physical gas sensors. Accordingly, we need four virtual sensor responses. As discussed, to classify the considered gases/odors, only the approximated steady-state responses determined by taking the average of static responses have been used. Henceforth, applying the padding of non-zero virtual sensor responses, each data vector in both datasets contains nine hybrid responses (physical and padded virtual sensor responses). These hybrid data vectors are restructured into the 2D-squared array having the shape (3×3). Thus, the obtained data vectors are further upscaled using mirror mosaicking. Consequently, we get the data vectors with dimensions augmented by three times. Subsequently, these data vectors having shapes (9×9) are used to train the simplified 2D-CNN. A step-wise flowchart for the procedure described above is given in Fig. 4.8.

4.5 Results and Discussion

We have used the already discussed simplified 2D-CNN to classify both datasets. While classifying both datasets, the same parameters have been used. The performance of simplified 2D-CNN has been obtained while testing it on 128 and 19 unknown test samples, respectively, for Dataset-1 and Dataset-2. Interestingly, we achieved well-classified results with an accuracy of 100% for both datasets. Hence, the achieved outperformance proves the efficacy of our proposed methodology. Our

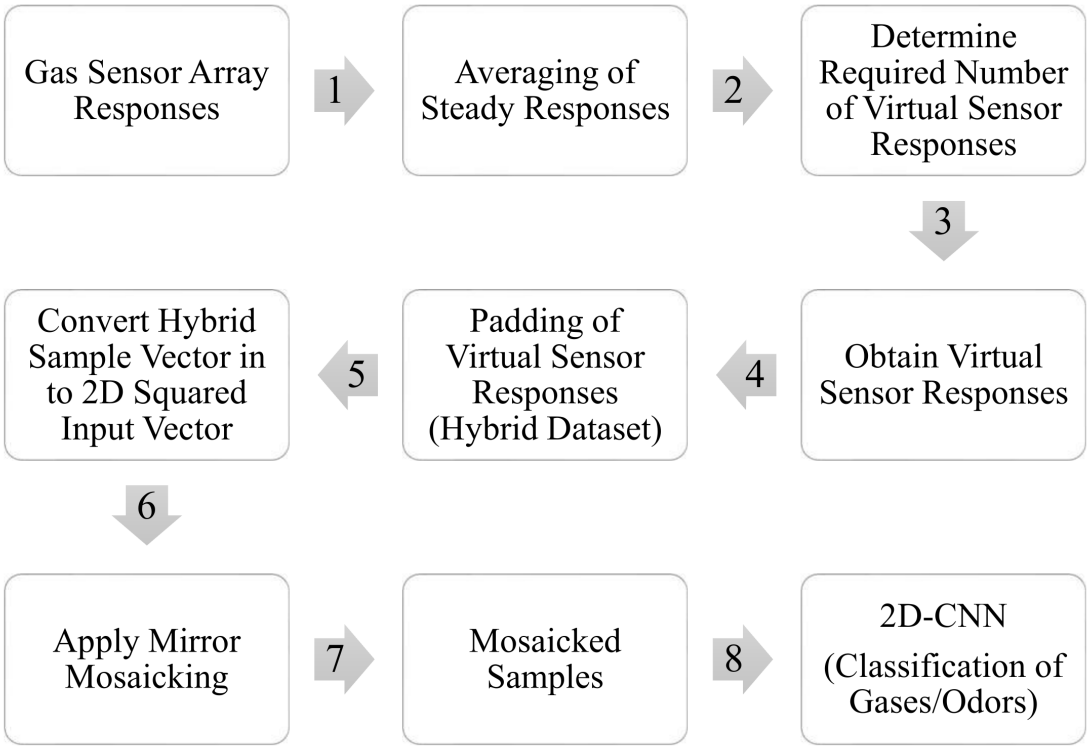

FIGURE 4.8: Step-wise Flowchart for Approach Implementation

approach not only classifies the target gases/odors but also classify the binary mixture that is non-linearly correlated. To demonstrate the effectiveness of novel non-zero padding of non-zero virtual sensor responses, we have compared the results obtained using conventional zero-padding. While using the zero-padding, the performance is taken as a baseline for comparison. However, non-zero virtual sensor responses can be obtained using various mathematical or statistical algorithms. Still, principal components provide dual advantages: non-zero virtual sensor responses and prioritization of principal components that bypass the need for feature selection. While using zero and non-zero virtual sensor responses, the obtained performances for gas/odor classification have been shown in Table 4.4. These performances have been assessed based on three metrics, viz., overall classification accuracy (OCA), kappa coefficient (K), and mean squared error (MSE). Also, the mathematical expressions associated with these performance metrics have been shown by equations

(4.1)-(4.3).

$$OCA = \frac{\sum_{i=1}^{C} G_{ii}}{\sum_{i,j=1}^{C} G_{ij,i\neq j}} \tag{4.1}$$

$$K = \frac{N\sum_{i=1}^{C} G_{ii} - \sum_{i=1}^{C} G_{i,act}G_{i,pred}}{N^2 - \sum_{i=1}^{C} G_{i,act}G_{i,pred}} \tag{4.2}$$

$$MSE = \frac{1}{N}\sum_{i=1}^{C}(G_{i,act} - G_{i,pred})^2 \tag{4.3}$$

where C is the number of target gases/odors, G_{ij} represents the number of well-classified samples $\forall(i = j)$ and misclassified samples $\forall(i \neq j)$. Moreover, $G_{i,act}$ and $G_{i,pred}$ are the actual and predicted target (gas/odor).

TABLE 4.4: Gases/Odors' Classification Performances While Using Zero and Non-Zero Virtual Sensor Responses

Metrics	Zero-Padded Virtual Sensor Responses	Principal Components-Padded Virtual Sensor Responses	Performance Enhancement
Dataset-1 (8 Physical and 1 Virtual Sensor Responses)			
OCA (%)	96.88	100	3.12
K	0.96	1.00	0.04
MSE	1.41×10^{-2}	7.75×10^{-3}	6.35×10^{-3}
Training Time (s)	19.232	23.855	
Dataset-2 (5 Physical and 4 Virtual Sensor Responses)			
OCA (%)	94.74	100	5.26
K	0.93	1.00	0.07
MSE	5.40×10^{-2}	4.20×10^{-2}	1.20×10^{-2}
Training Time (s)	1.027	1.133	
$(OCA : OverallClassificationAccuracy)$ $(K : KappaCoefficient)$ $(MSE : MeanSquaredError)$			

Our proposed approach's outperformance indicates that the classification of considered gases/odors can be achieved using a simplified 2D-CNN even using approximated steady-state responses with PC-based non-zero virtual sensor responses. Moreover, our proposed approach can achieve competitive classification results even using conventional zero-padding-based virtual sensor responses. However, using PC-based non-zero virtual sensor responses instead of conventional zero-padding, the significant performance enhancement can be observed in Table 4.4. Also, our approach depicts the generalizability that enables us to use other virtual sensor responses derived from various normalization and transformation techniques. Therefore, we can apply the proposed novel approach in multiple domains of state-of-the-art research.

The justification for using principal components analysis instead of other normalization and transformation techniques is that it generates principal components with an inherent ranking based on information variance. The inherent ranking solves the issue of selecting virtual sensor responses as per requirement. While requiring the virtual sensor responses, we need at least one essentially. Fortunately, the first principal component has most of the information variance of data. In contrast, the components of conventional zero-padding provide no information. With the results, performance enhancement while using non-zero (PC-based) virtual sensor responses can be seen through each of the metrics. Also, non-zero values represent more information to the CNN, which eventually enhances the classification results. In the case of dataset-2, we achieve well-classified results even using a truncated dataset instead of all the responses from 16 physical gas sensors. While evaluating the trained simplified 2D-CNN on unknown test samples from both datasets, we have achieved 100% correct classification.

4.6 Conclusion

Designing the electronic noses (e-Noses) using several gas sensor elements in a gas sensor array has been a traditional approach in gas sensing. There is no thumb rule in the literature to fix the optimal number of gas sensor elements. However, for gas/odor classification, high performance can be achieved using multiple physical gas sensors, which is impractical for cost and power-efficient applications. It is also unsuitable for miniaturized system-on-chip (SoC). Artificial Neural Networks (ANN) and other conventional pattern recognition methods have also been quite popular for classifying the gases/odors using transient and steady-state responses of the gas sensor array. A vast literature witnesses the outperformance of ANNs over their peers. But ANNs are also computationally complex due to the usage of only fully-connected or dense layers. However, in the modern era, 6G-driven Internet of Things (6G-IoTs) applications require an ultra low-powered sensor array without compromising performance. Nowadays, CNNs are being used to design e-Noses that embed edge intelligence on the gas sensor node compatible with modern technology. But CNNs have been used to classify the gases/odors using only transient responses. In contrast, no original work has been found using CNNs on steady-state responses. Hence, we have proposed a novel approach that leverages CNNs to classify the gases/odors using steady-state responses. To accomplish this task, we upscale the raw data vectors derived from steady-state responses two times using the concept of non-zero virtual sensor responses and mirror mosaicking. Thus, modified upscaled data vectors are called hybrid responses (physical and virtual sensor responses). While classifying the datasets by a simplified 2D-CNN using the upscaled hybrid data vectors, we have been able to achieve 100% accuracy for both dataset-1 and dataset-2.

With this 100% classification accuracy over the chosen test samples, NOT used during the training of the CNNs, our results outperform the previously published results on the same datasets. Aforesaid non-zero virtual sensor responses are derived from principal component analysis. It is also evident that a simplified 2D-CNN can outperform even using much less information if the same information could be presented with more diversity like our approach. Accordingly, various normalization and transformation techniques can be explored to provide more robust performance. It can also be noted that the gas sensor elements consume significantly high power on the sensor node, and utilizing more virtual sensor responses instead of real-physical sensors will substantially reduce the power requirements of the sensor node. To the best of the authors' knowledge, this work is the first of its kind.